

## References and Notes

- (1) S. Shankman and A. R. Gordon, *J. Am. Chem. Soc.*, **61**, 2370 (1939).
- (2) R. H. Stokes, *J. Am. Chem. Soc.*, **69**, 1291 (1947); *Trans. Faraday Soc.*, **44**, 295 (1948).
- (3) W. H. Beck, K. P. Singh, and W. F. K. Wynne-Jones, *Trans. Faraday Soc.*, **55**, 331 (1959).
- (4) W. H. Beck, J. V. Dobson, and W. F. K. Wynne-Jones, *Trans. Faraday Soc.*, **56**, 1172 (1960).
- (5) W. F. Glauque, E. W. Hornung, J. E. Kunzler, and T. R. Rubin, *J. Am. Chem. Soc.*, **82**, 62 (1960).
- (6) J. A. Duisman and W. F. Glauque, *J. Phys. Chem.*, **72**, 562 (1968).
- (7) K. S. Pitzer, *J. Phys. Chem.*, **77**, 268 (1973).
- (8) K. S. Pitzer and G. Mayorga, *J. Phys. Chem.*, **77**, 2300 (1973); **78**, 2698 (1974).
- (9) K. S. Pitzer and J. J. Kim, *J. Am. Chem. Soc.*, **96**, 5701 (1974).
- (10) W. J. Hamer, "The Structure of Electrolytic Solutions", Wiley, New York, N.Y., 1959, Chapter 15.
- (11) K. S. Pitzer and L. Brewer, "Thermodynamics", Revised edition, G. N. Lewis and M. Randall, Ed., McGraw-Hill, New York, N.Y., 1961, pp 587-590.
- (12) K. S. Pitzer and L. F. Silvester, *J. Solution Chem.*, **5**, 269 (1976).
- (13) T. L. Hill, "Introduction to Statistical Mechanics", Addison-Wesley, Reading, Mass., 1960, Chapter 19.
- (14) A. K. Covington, J. V. Dobson, and W. F. K. Wynne-Jones, *Trans. Faraday Soc.*, **61**, 2050 (1965).
- (15) J. Shrawder, Jr., and I. A. Cowperthwaite, *J. Am. Chem. Soc.*, **56**, 2340 (1934).
- (16) T. H. Lilley and C. C. Briggs, *Electrochim. Acta*, **20**, 257 (1975).
- (17) K. S. Pitzer, *J. Phys. Chem.*, **80**, 2863 (1976).
- (18) W. J. Hamer, *J. Am. Chem. Soc.*, **57**, 9 (1935).
- (19) H. S. Harned and W. J. Hamer, *J. Am. Chem. Soc.*, **57**, 27 (1935).
- (20) S. A. Brown and J. E. Land, *J. Am. Chem. Soc.*, **79**, 3015 (1957).
- (21) E. Lange, J. Monheim, and A. L. Robinson, *J. Am. Chem. Soc.*, **55**, 4733 (1933).
- (22) J. E. Kunzler and W. F. Glauque, *J. Am. Chem. Soc.*, **74**, 3472 (1952).
- (23) W. L. Groenier, Thesis, University of Chicago, 1936.
- (24) Y. C. Wu, Thesis, University of Chicago, 1957.
- (25) K. S. Pitzer, *J. Am. Chem. Soc.*, **59**, 2365 (1937).
- (26) J. M. Austin and A. D. Malr, *J. Phys. Chem.*, **66**, 519 (1962).
- (27) V. S. K. Nair and G. H. Nancollas, *J. Chem. Soc.*, 4144 (1958); see also C. W. Davies, H. W. H. Jones, and C. B. Monk, *Trans. Faraday Soc.*, **48**, 921 (1952).
- (28) H. S. Dunsmore and G. H. Nancollas, *J. Phys. Chem.*, **68**, 1579 (1964).
- (29) A. K. Covington, J. V. Dobson, and W. F. K. Wynne-Jones, *Trans. Faraday Soc.*, **61**, 2057 (1965).
- (30) R. A. Robinson and R. H. Stokes, "Electrolytic Solutions", Butterworths, London, 1959.
- (31) J. A. Rard, A. Habenschuss, and F. H. Spedding, *J. Chem. Eng. Data*, **21**, 374 (1976).
- (32) K. S. Pitzer, *J. Chem. Soc., Faraday Trans. 2*, **68**, 101 (1972).
- (33) T. F. Young, L. F. Maranville, and H. M. Smith, "The Structure of Electrolytic Solutions", W. J. Hamer, Ed., Wiley, New York, N.Y., 1959, Chapter 4.
- (34) M. Kerker, *J. Am. Chem. Soc.*, **79**, 3664 (1957).
- (35) D. D. Wagman et al., *Natl. Bur. Stand. (U.S.), Tech. Note*, 270-3 (1968).
- (36) K. Gallagher, G. E. Brodale, and T. E. Hopkins, *J. Phys. Chem.*, **64**, 687 (1960).
- (37) P. F. Meads, W. R. Forsythe, and W. F. Glauque, *J. Am. Chem. Soc.*, **63**, 1902 (1941).
- (38) CODATA, Tentative set of key values for thermodynamics, Part IV (1974).
- (39) R. G. Bates, M. Edelstein, and S. F. Acree, *J. Res. Natl. Bur. Stand.*, **36**, 159 (1946).
- (40) S. R. Gupta, G. J. Hillis, and D. J. G. Ives, *Trans. Faraday Soc.*, **59**, 1874 (1963).
- (41) L. F. Silvester and K. S. Pitzer, Lawrence Berkeley Laboratory Report No. 4456 (1976), to be published.
- (42) H. K. J. Powell, *J. Chem. Soc., Dalton Trans.*, 1947 (1973).
- (43) S. Cabani and P. Gianni, *Anal. Chem.*, **44**, 253 (1972).

## Qualitative Potential Energy Surfaces. 5. Sigmatropic Shifts

N. D. Epiotis\* and S. Shaik

*Contribution from the Department of Chemistry, University of Washington,  
Seattle, Washington 98195. Received December 15, 1975*

**Abstract:** The LCFC approach is used to generate the manifold of PE surfaces for radical-radical combination reactions and sigmatropic shifts. The effect of polarity on reaction rate and reaction toposelectivity is discussed. It is predicted that (a) within a series of structurally similar compounds, the rate of an  $i,j$  thermal sigmatropic shift increases as the migration framework and the migration group become a better donor-acceptor pair and (b) a thermal or photochemical sigmatropic shift occurs in the topochemical manner which couples the best donor-acceptor combination of migration framework and migrating group. Experimental data which support the qualitative theory are presented.

In previous papers,<sup>1</sup> we have explored how the linear combination of fragment configurations (LCFC) method can be used to construct qualitative potential energy (PE) surfaces for various classes of chemical reactions. In this paper, we extend our approach to sigmatropic shifts after a background discussion of the LCFC qualitative PE surfaces for radical-radical combination reactions.

### (I) Potential Energy Surfaces for Radical-Radical Combination Reactions

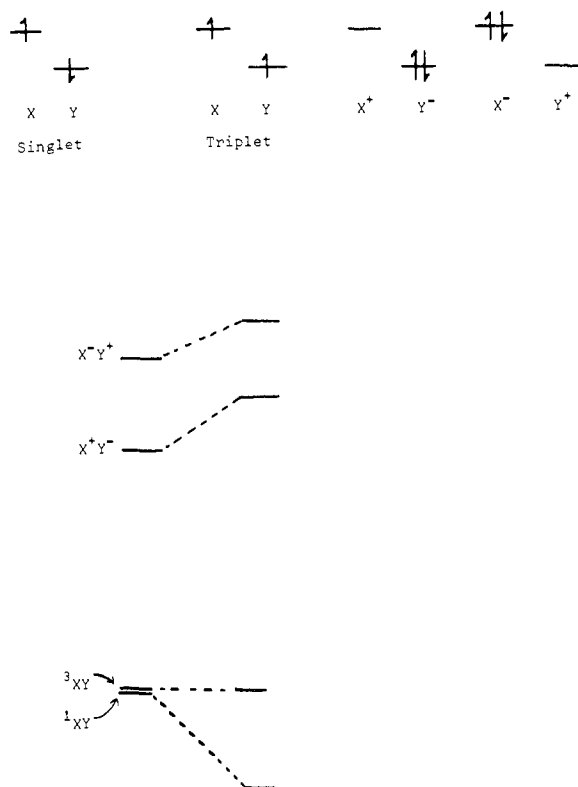
We first consider covalent bond formation from a singly occupied X AO and a singly occupied Y AO by reference to the static LCFC diagram shown in Figure 1. The following important trends should be noted: (a) The ground state of the bond has a dominant no bond contribution while the lowest excited state is primarily ionic. (b) The mixing of the no bond and lowest charge transfer configurations, and, hence, X-Y bond strengths, is expected to increase as the ionization potential of one singly occupied AO decreases, the electron affinity of the other singly occupied AO increases, and the corresponding interaction matrix element increases. This situation

is illustrated by the greater bond dissociation energy of  $\text{CH}_3\text{-F}$  as compared with that of  $\text{CH}_3\text{-H}$ . However, in situations where an increase of the polarity of the system is counteracted by a "shrinkage" of the AO coefficients of the uniting centers, reduction of the absolute magnitude of the interaction matrix element may dominate the diminution of the energy gap separating the interacting DA and  $\text{D}^+\text{A}^-$  configurations. The smaller C-H bond dissociation energy of  $\text{PhCH}_2\text{-H}$  as compared with that of  $\text{CH}_3\text{CH}_2\text{CH}_2\text{-H}$  can be traced to such conflicting trends. The two contrasting cases are illustrated in Figure 2.

The comparison of  $\text{CH}_3\text{CH}_2\text{CH}_2\text{-H}$  and  $\text{PhCH}_2\text{-H}$  dissociation energies is instructive and merits attention.

	Donor (D)	Acceptor (A)	$I_D - I_A$ , eV	$\langle \text{DA}   \hat{P}   \text{D}^+\text{A}^- \rangle$ (in kS units)
$\text{CH}_3\text{CH}_2\text{-CH}_2\text{-H}$	$\text{CH}_3\text{CH}_2\text{CH}_2\cdot$	$\text{H}\cdot$	~7.0	~1.00
$\text{PhCH}_2\text{-H}$	$\text{PhCH}_2\cdot$	$\text{H}\cdot$	~6.5	0.76

Increased delocalization in D leads to increased polarity cou-



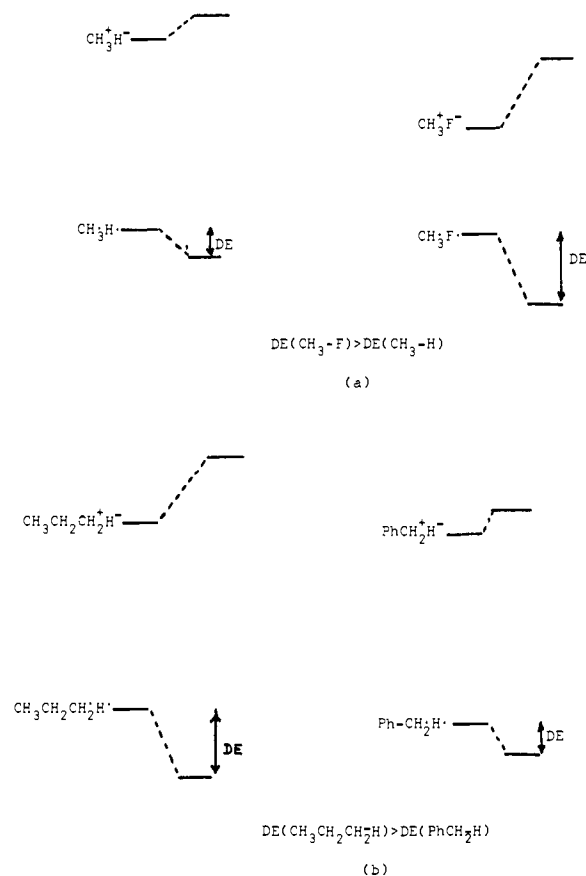
**Figure 1.** Basis set configurations and static LCFC diagram describing the bond states for two singly occupied AO's centered on X and Y.

pled with an orbital electron density "dilution" effect. Hence, the polarity effect may favor a stronger C-H bond in PhCH<sub>2</sub>-H while the associated matrix element effect favors a stronger C-H bond in CH<sub>3</sub>CH<sub>2</sub>CH<sub>2</sub>-H. When spatial orbital overlap is strong, matrix element control is imposed and the result is a smaller bond dissociation energy in the case of PhCH<sub>2</sub>-H. This reflects the orbital electron density "dilution" effect present in this system which, in turn, is connected to  $\pi$  conjugation in the formal PhC $\dot{C}$ H<sub>2</sub> radical. (c) The above description is applicable to any covalent  $\sigma$  or  $\pi$  bond. An ionic bond will be formed when the D<sup>+</sup>A<sup>-</sup> configuration drops below the DA configuration. Obviously, this will occur when the singly occupied X has a very low ionization potential and the singly occupied Y a substantial electron affinity, e.g., NaCl.

Next, we shall consider the surface manifold for the reaction of two atoms or radicals to form a  $\sigma$  covalently bonded or an ionically bonded molecule. The symbols DA, D<sup>+</sup>A<sup>-</sup>, and D<sup>-</sup>A<sup>+</sup> have their usual meaning<sup>1</sup> and the diabatic and adiabatic surfaces which obtain in the two cases are shown in Figures 3 and 4. Once again, polar solvents may lead to a situation where a nonionic reaction is rendered ionic by virtue of the stabilization of the  $\Phi_2$  adiabatic surface which can now cross the  $\Phi_1$  adiabatic surface. Unimolecular solvolytic reactions are such cases.

In describing a simple radical combination reaction, one has to note that the steric function of the no bond, monoexcited, etc., diabatic surface equations will be very small simply because significant bond readjustment is not required, i.e., the two radicals may coalesce to form a product in nearly a frozen geometrical state. This is, of course, rigorously valid for atom combination reactions and a fair approximation for alkyl and aryl radical combination reactions. Accordingly, since the DA diabatic surface will be nearly flat, the activation energies for radical combination reactions are expected to be near zero. This is, indeed, what is observed experimentally.<sup>2</sup>

The effect of reaction polarity on an intrinsically very low barrier height is expected to be very small. Indeed, it is found



**Figure 2.** (a) Energy gap control of bond dissociation energy (DE). (b) Matrix element control of bond dissociation energy (DE).

**Table I.** Termination Rate Constants for Alkyl Radicals in Solution<sup>a</sup>

Radical	Solvent	Approx rel rates	$I - A$ , eV
H- $\dot{C}H_2$	Cyclohexane	1.0	8.8
Me- $\dot{C}H_2$	Ethane	0.7	8.1
Et- $\dot{C}H_2$	Cyclohexane	0.4	7.3
Ph- $\dot{C}H_2$	Benzene	0.4	6
(Me) <sub>2</sub> $\dot{C}$ -H	Benzene	1.0	7.3
(Me) <sub>2</sub> $\dot{C}$ -CN	Benzene	0.1	7.3
(Me) <sub>2</sub> $\dot{C}$ -Ph	Benzene	0.8	5.9
(Me) <sub>3</sub> $\dot{C}$	Cyclohexane	1.0	7.0
(Me) <sub>3</sub> Si	Cyclohexane	1.0	
(Me) <sub>3</sub> Sn	Cyclohexane	1.4	

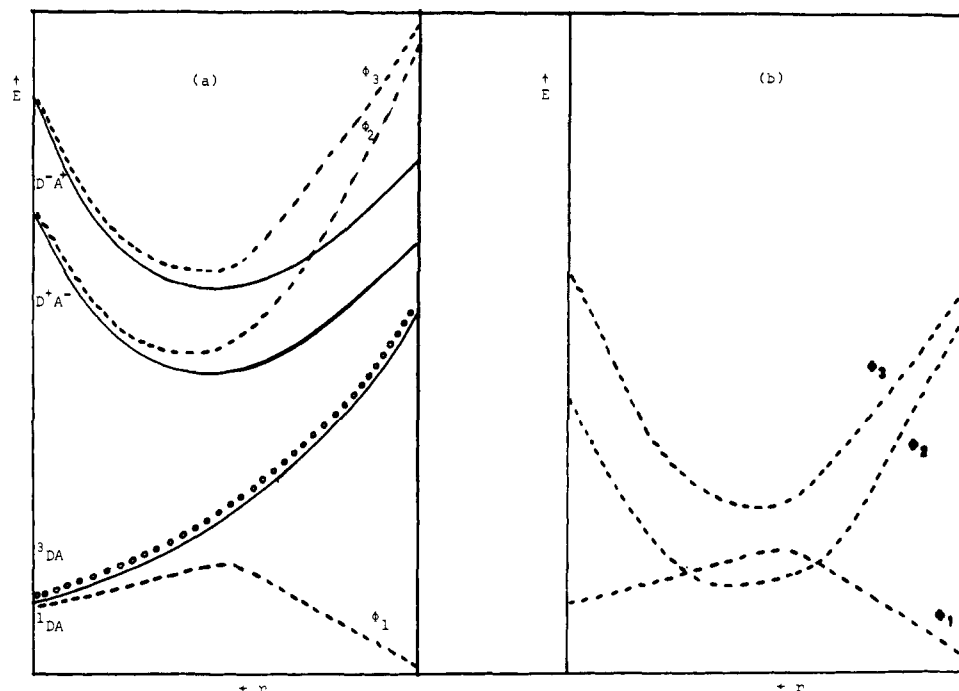
<sup>a</sup>D. C. Nonhebel and J. C. Walton, "Free Radical Chemistry", Cambridge University Press, London, 1974.

experimentally that most rate constants for alkyl radical combinations are within a factor of 10. Typical examples are collected in Table I.

In the case of ionic atom combination reactions, the crossing of DA and D<sup>+</sup>A<sup>-</sup> diabatic surfaces occurs very early on the reaction coordinate and the barrier is practically zero. This situation is typical of the union of Na and Cl to form Na<sup>+</sup>Cl<sup>-</sup> (Figure 4).

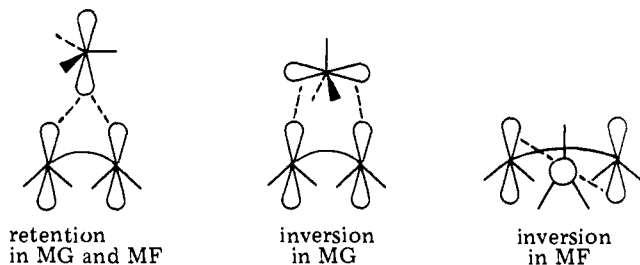
## (II) Potential Energy Surfaces for Sigmatropic Shifts

A successful theory of sigmatropic shifts has to account satisfactorily for the following reaction features:

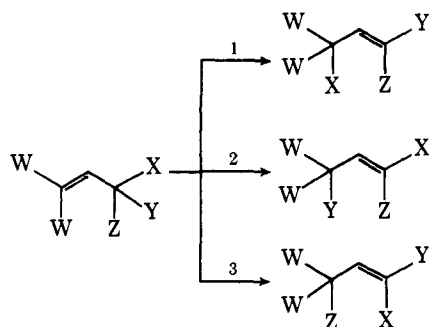


**Figure 3.** (a) Diabatic (solid lines) and adiabatic (dashed lines) PE surfaces describing the interaction of two atoms or radicals to form a bond. Triplet adiabatic surface is indicated by open circles. (b) The readjustment of the singlet adiabatic surfaces under the influence of polar solvents, e.g., solvolytic reactions.

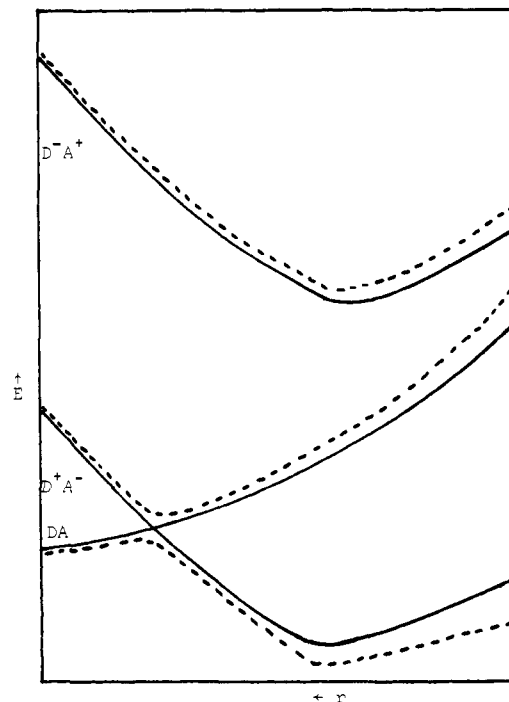
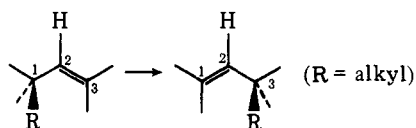
(a) Stereoselectivity. For reasons which will become clear later, we can restrict our attention to two different types of reaction modes: shifts occurring by retention of configuration in both migrating group (MG) and migrating framework (MF) and shifts occurring by inversion of configuration in either MG or MF. Examples are shown below:



(b) Toposelectivity. Sigmatropic shifts are intriguing since, in most systems, more than one reaction pathway is available.



(c) The effect of polarity [ $I_D - A_A$ ] on reaction rates. We shall illustrate our approach by reference to the model reaction shown below:



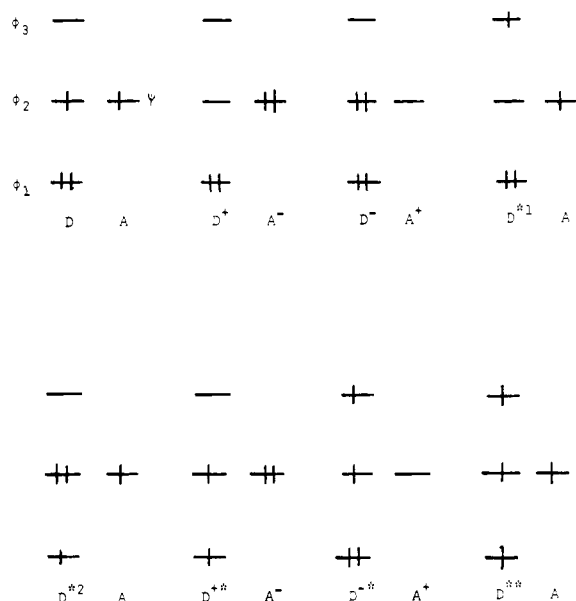
**Figure 4.** Diabatic (solid lines) and adiabatic (dashed lines) PE surfaces describing the interaction of two atoms or radicals to form an ionic bond.

We shall restrict our attention to two stereochemical paths, one involving suprafacial migration with retention of configuration and the other suprafacial migration with inversion of configuration of the MG. These two different stereochemical paths will be designated SR and SI. The basis set configurations are shown in Figure 5. The equations of the diabatic surfaces are given below:<sup>3</sup>

$$E(DA) \approx S \quad (1)$$

**Table II.** Interaction Matrix for 1,3-Sigmatropic Shift

	DA	D <sup>+</sup> A <sup>-</sup>	D <sup>-</sup> A <sup>+</sup>	D* <sup>1</sup> A	D* <sup>2</sup> A	D** <sup>+</sup> A <sup>-</sup>	D** <sup>-</sup> A <sup>+</sup>	D**A
DA		( $\phi_2 - \psi$ )	( $\phi_2 - \psi$ )	0	0	( $\phi_1 - \psi$ )	( $\phi_3 - \psi$ )	0
D <sup>+</sup> A <sup>-</sup>			0	( $\phi_3 - \psi$ )	0	0	0	0
D <sup>-</sup> A <sup>+</sup>				0	( $\phi_1 - \psi$ )	0	0	0
D* <sup>1</sup> A					0	0	( $\phi_2 - \psi$ )	0
D* <sup>2</sup> A						( $\phi_2 - \psi$ )	0	0
D** <sup>+</sup> A <sup>-</sup>							0	( $\phi_3 - \psi$ )
D** <sup>-</sup> A <sup>+</sup>								0
D**A								

**Figure 5.** Basis set configurations for the treatment of a 1,3-sigmatropic shift.

$$E(D^+A^-) \approx I_D - A_A + C + S' \quad (2)$$

$$E(D^-A^+) \approx I_A - A_D + C' + S' \quad (3)$$

$$E(D^*1A) \approx {}^2G(\phi_2 \rightarrow \phi_3) + S' \quad (4)$$

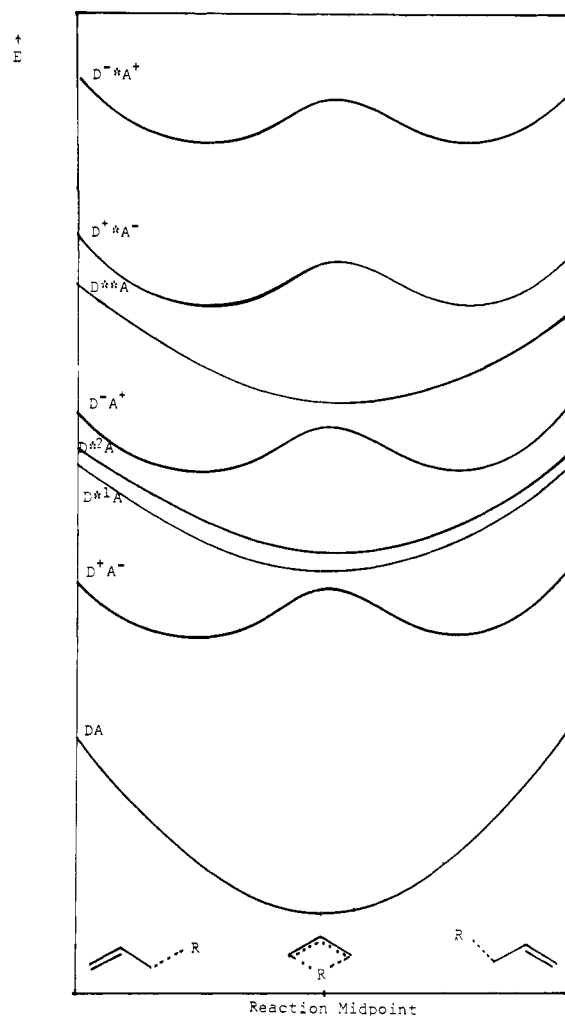
$$E(D^*2A) \approx {}^2G(\phi_1 \rightarrow \phi_2) + S' \quad (5)$$

$$E(D^{**+}A^-) \approx I_D - A_A + {}^1G(\phi_1 \rightarrow \phi_2) + C'' + S'' \quad (6)$$

$$E(D^{**+}A^+) \approx I_A - A_D + {}^1G(\phi_2 \rightarrow \phi_3) + C''' + S'' \quad (7)$$

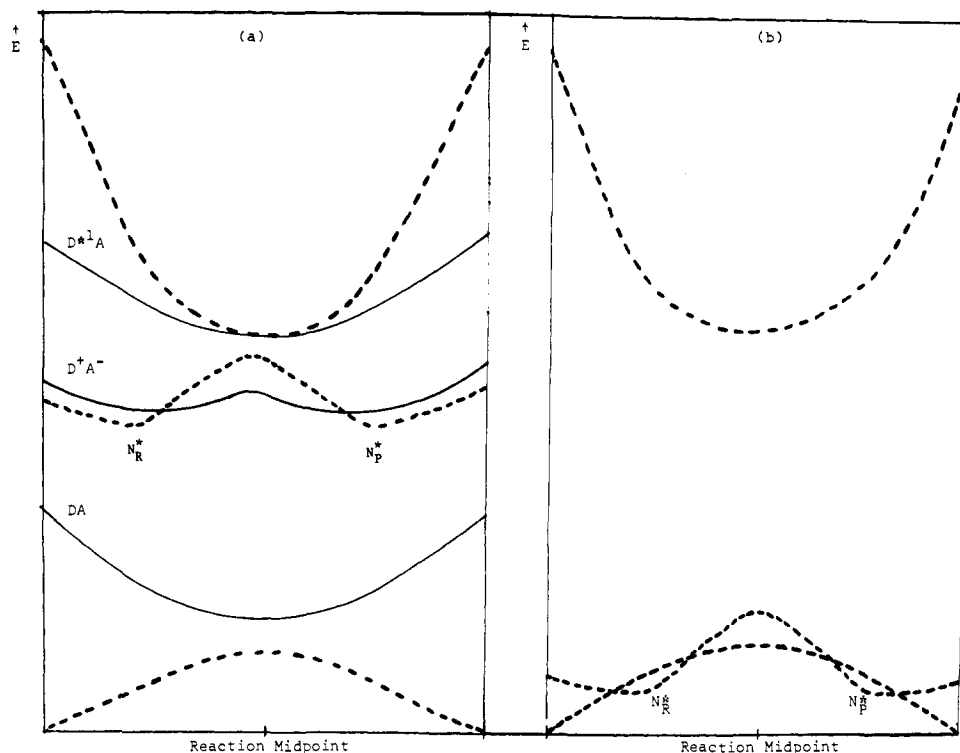
$$E(D^{**}A) \approx {}^2G(\phi_1 \rightarrow \phi_3) + S'' \quad (8)$$

The interaction matrix is shown in Table II. Unlike intermolecular reactions, these matrix elements change continuously as a function of the geometry of the reaction complex. Thus, for example, when the MG is near one of the termini of the MF, only bicentric interactions need be considered and one-electron interaction matrix elements are large, irrespective of the stereochemistry of the migration. By contrast, at the reaction midpoint, the interaction matrix elements become characteristic of the stereochemical path. Thus, it becomes apparent that near the beginning or end of the rearrangement process, all diabatic surfaces will interact strongly, irrespective of the stereochemical path. By contrast, at the reaction midpoint, the strength of these interactions will critically depend upon the nature of the stereochemical path. Accordingly, a determination of the preferred reaction path can be made from mere consideration of the electronic states at the reaction midpoint. Hence, we can simplify the discussion of sigmatropic shifts by adopting a static model and utilizing static LCFC diagrams. This approach has been described in an older publication.<sup>4</sup>

**Figure 6.** Diabatic PE surfaces for the treatment of 1,3-sigmatropic shift.

The diabatic surfaces describing the motion of the MG from its initial or final point of attachment to the reaction midpoint resemble the diabatic surfaces encountered in the case of covalent bond dissociation. This can be best understood by reference to the model 1,3-sigmatropic shift. Specifically, accumulation of nuclei is maximal at the initial and final stages of the rearrangement and minimal at the reaction midpoint. Since steric repulsion parallels nuclear accumulation, the DA diabatic surface has the shape shown in Figure 6. In addition, steric repulsion and coulombic attraction between MF<sup>+</sup> and MG<sup>-</sup> (or MF<sup>-</sup> and MG<sup>+</sup>) is minimal at the reaction midpoint and maximal at the initial or final rearrangement stages. Since coulombic attractive effects predominate at long or modest interfragment distances and steric repulsive effects take over at short interfragment distances, the D<sup>+</sup>A<sup>-</sup> and D<sup>-</sup>A<sup>+</sup> diabatic surfaces have the shape shown in Figure 6.

The energy ordering of the diabatic surfaces depends on the



**Figure 7.** (a) Diabatic (solid lines) and adiabatic (dashed lines) PE surfaces for a 1,3-sigmatropic shift proceeding by inversion. (b) The readjustment of the adiabatic surfaces under the influence of polar solvent.

polarity, i.e., as the MG and the MF become a better donor-acceptor pair, the  $D^+A^-$  curve is translated downwards whereas the  $D^-A^+$  curve is translated upwards in energy. Similar considerations apply to the charge excited diabatic surfaces. In highly polar systems, the  $D^+A^-$  curve will cross the  $DA$  curve, marking a change from nonionic to ionic sigmatropic shift.

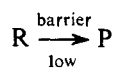
An inspection of the interaction matrix suggests the following simplifications in constructing adiabatic PE surfaces of sigmatropic shifts:

(a) Adiabatic PE surfaces for suprafacial 1,3 shifts proceeding by inversion can be constructed by using the  $DA$ ,  $D^+A^-$ , and  $D^*A^-$  diabatic surfaces (Figure 7).

(b) Adiabatic PE surfaces for suprafacial 1,3 shifts proceeding by retention can be constructed by using the  $DA$ ,  $D^+A^-$ ,  $D^*A^-$ , and  $D^*A^-$  diabatic surfaces (Figure 8).

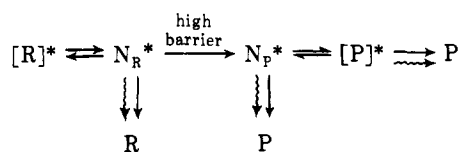
The mechanistic implications of the adiabatic PE surfaces can be conveyed by the following chemical equations, where a wavy line signifies radiationless decay:

(a) Thermal 1,3-sigmatropic shift (SI path)

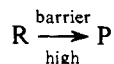


R = reactant; P = product

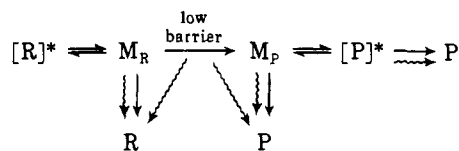
(b) Singlet photochemical 1,3-sigmatropic shift (SI path).<sup>5</sup>



(c) Thermal 1,3-sigmatropic shift (SR path).



(d) Singlet photochemical 1,3-sigmatropic shift (SR path).<sup>6</sup>



Note that the terms "high" and "low" barrier refer exclusively to electronic effects.

The most important mechanistic conclusions are the following:

(a) Assuming comparable spatial overlap and steric interactions of the MF and MG, the thermal SI barrier will be lower than the thermal SR barrier due to a stronger  $DA-D^+A^-$  interaction as compared with the  $DA-D^*A^-$  interaction. However, once it is realized that steric effects operate in favor of the SR path, it is clear that the relative barrier heights for the two stereochemical migration modes will be determined by a balance of electronic and steric effects.

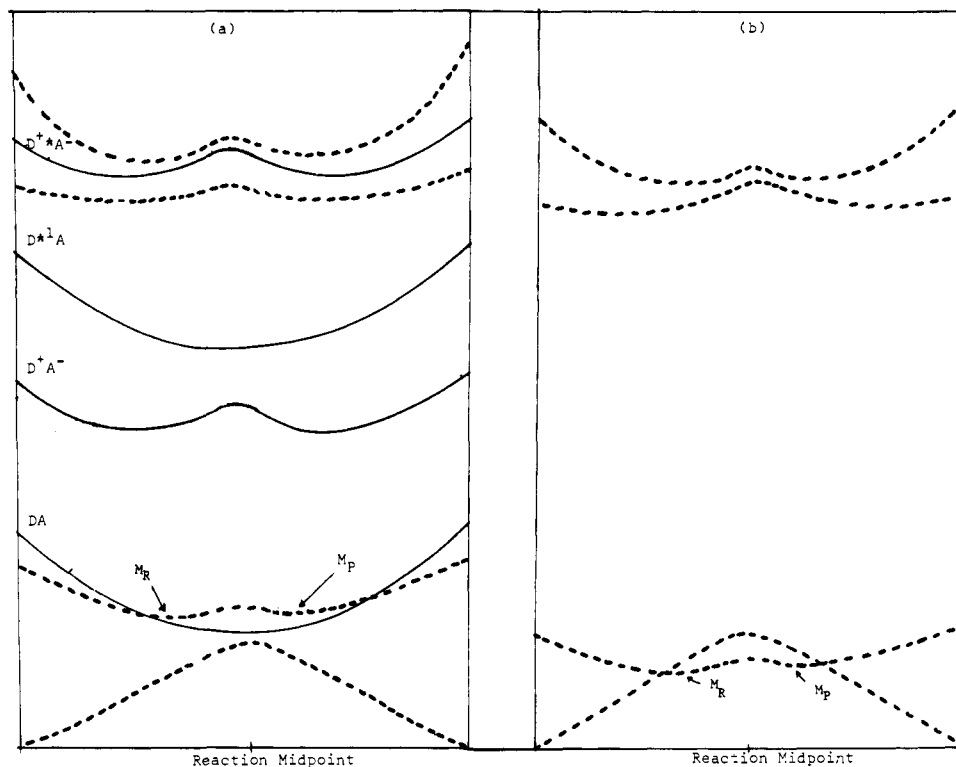
(b) Both SI and SR thermal paths involve pericyclic bonding. Accordingly, and depending upon the balance of electronic and steric effects, a 1,3-sigmatropic shift may be SR stereoselective, SI stereospecific, or nonstereoselective due to competition of pericyclic SR and SI mechanisms.

(c) The SR photochemical barrier is lower than the SI photochemical barrier due to the fact that  $D^+A^-$  interacts with higher lying diabatic surfaces but not with the lower lying  $DA$  diabatic surface. For similar reasons, the energy gap separating the ground and the first excited surface about the reaction midpoint is much smaller in the case of the SR path. Accordingly, both barrier as well as decay considerations<sup>7</sup> suggest that the SR photochemical mechanism will be preferred over the SI photochemical mechanism.

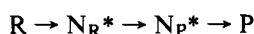
(d) Both SR and SI photochemical pathways involve excited unsymmetrical intermediates albeit of different electronic nature.<sup>5,6</sup>

The effect of polar solvent on the mechanism of [1,3]-sigmatropic shifts is illustrated in Figures 7 and 8 and is conveyed by means of the following equations:<sup>8</sup>

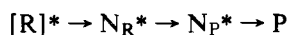
(a) Thermal 1,3-sigmatropic shift (SI path)



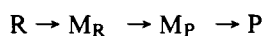
**Figure 8.** (a) Diabatic (solid lines) and adiabatic (dashed lines) PE surfaces for a 1,3-sigmatropic shift proceeding by retention. (b) The readjustment of the adiabatic surfaces under the influence of polar solvents.



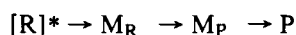
(b) Photochemical 1,3-sigmatropic shift (SI path).



(c) Thermal 1,3-sigmatropic shift (SR path).



(d) Photochemical 1,3-sigmatropic shift (SR path).

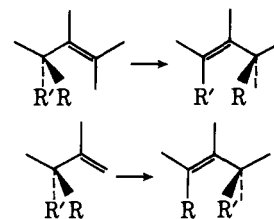


A typical example of a sigmatropic shift occurring in a polar solvent is provided by the solvolysis of allylic halides. The elegant work of Snee has demonstrated the existence of two interconvertible unsymmetrical ion pair intermediates in the allylic rearrangement.<sup>9</sup> These results are in good agreement with mechanistic predictions regarding this reaction based on the PE surfaces of Figures 7 and 8.

The analysis presented for the model 1,3-sigmatropic shift can be extended to any *i,j*-sigmatropic shift in the manner indicated below.

No. of electrons	Stereochemical path	PE surfaces
4 <i>N</i>	SR	Figure 8
4 <i>N</i>	SI	Figure 7
4 <i>N</i> + 2	SR	Figure 7
4 <i>N</i> + 2	SI	Figure 8

**(A) Toposelectivity of Sigmatropic Shifts.** The toposelectivity of a sigmatropic shift occurring within one molecule and the relative rate of two sigmatropic shifts occurring in two different molecules are intimately related problems. For example, consider the two reactions shown below, each one assumed to occur via an SI stereochemical path. We further assume that in both cases the allyl MF acts as the acceptor partner and the MG as the donor partner, with R' being a better donor than R. In other words, we wish to compare the activation energies of two reactions, D + A and D' + A, where the latter has



higher polarity. In doing so, one should consider the following:

(a) The interaction of the DA and D<sup>+</sup>A<sup>-</sup> diabatic surfaces vs. that of the D'A and D'<sup>+</sup>A<sup>-</sup> surfaces at the initial stage of the rearrangement, i.e., near covalent bonding of the two fragments. In this case, orbital overlap is very strong and small differences in polarity can be overcompensated by differences in matrix elements. In general, the operation of the orbital electron density "dilution" effect renders the matrix element controlled interaction of DA and D<sup>+</sup>A<sup>-</sup> superior to that of D'A and D'<sup>+</sup>A<sup>-</sup>, i.e., weaker bonding accompanies greater polarity. As a result, a bond strength effect favors a more facile migration of R'.

(b) The interaction of the DA and D<sup>+</sup>A<sup>-</sup> diabatic surfaces vs. that of the D'A and D'<sup>+</sup>A<sup>-</sup> surfaces at the reaction midpoint. In this case, spatial orbital overlap is weak and the effect of polarity becomes relatively more important. As a result, the inferiority of the D'A and D'<sup>+</sup>A<sup>-</sup> relative to the DA and D<sup>+</sup>A<sup>-</sup> interaction is reduced. Accordingly, the more polar reaction will be faster. The reader can verify that similar conclusions are valid if the two reactions occur via the SR stereochemical path.

On the basis of the above considerations, we can propose that  $I_D - A_A$  will be an index of the activation energy of a sigmatropic shift with the reaction barrier becoming lower as  $I_D - A_A$  decreases. Accordingly, relative rates as well as toposelectivity can be predicted in a simple manner.

A similar analysis can be given for the case of photochemical shifts. In this case, excitation will be preferentially localized

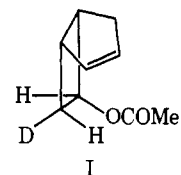
Table III. Activation Parameters of Thermal Sigmatropic Shifts

Reactant	Thermal product	$I - A, I$ eV	$E_a$ , kcal/mol	Log $A$ , s <sup>-1</sup>	Ref
		~5.08	28.6	10.38	<i>a</i>
		~5.28	30.6	11.70	<i>b</i>
		~5.61	34.2	10.55	<i>c</i>
		~5.61	35.3	10.39	<i>c</i>
		~6.7	32.5	10.80	<i>d</i>
		~7.0	$\Delta H^\ddagger = 35.4$		<i>e</i>
		~7.0	37.7	11.86	<i>e</i>
		~7.7	20.4		<i>f</i>
		~7.7	19.9		<i>g</i>
		~7.9	24.3	12.11	<i>h</i>
		~5.46	26.4	10	<i>i</i>
		≤5.86	27.6	10.8	<i>j</i>
		~5.86	31.5	11.2	<i>k</i>

<sup>a</sup>E. Foster, A. C. Cope, and F. Daniels, *J. Am. Chem. Soc.*, 69, 1893 (1947). <sup>b</sup>F. W. Schuler and G. W. Murphy, *ibid.*, 72, 3155 (1950). <sup>c</sup>H. M. Frey and R. K. Solly, *Trans. Faraday Soc.*, 64, 1858 (1968). <sup>d</sup>H. M. Frey and B. M. Pope, *J. Chem. Soc. A*, 1701 (1966). <sup>e</sup>W. R. Roth and J. König, *Justus Liebigs Ann. Chem.*, 699, 24 (1966). <sup>f</sup>S. McLean and P. Haynes, *Tetrahedron*, 21, 2329 (1965). <sup>g</sup>S. McLean, C. J. Webster, and R. J. D. Rutlerford, *Can. J. Chem.*, 47, 1555 (1969). <sup>h</sup>W. R. Roth, *Tetrahedron Lett.*, 1009 (1964). <sup>i</sup>T. Nozoe and K. Takahashi, *Bull. Chem. Soc. Jpn.*, 38, 665 (1965). <sup>j</sup>A. P. Ter Borg and H. Kloosterziel, *Recl. Trav. Chim. Pays-Bas.*, 82, 741 (1963). <sup>k</sup>A. P. Ter Borg, H. Kloosterziel, and N. Van Meurs, *ibid.*, 82, 717 (1963). <sup>l</sup> $I$  of  $\alpha$ -carbonylmethyl radical was estimated as 2.9 eV.  $I$  of pentadienyl radical was taken from: R. Zahradnik and P. Carsky, *Prog. Phys. Org. Chem.*, 10, 327 (1973).  $I$  of 1-methylpentadienyl radical was estimated as ~7.4 eV.  $I$  of cyclopentadienyl radical and cycloheptatrienyl radicals were taken from: A. Streitwieser, Jr., *Prog. Phys. Org. Chem.*, 1, 1 (1963).  $I$  of 1-methylcyclopentadienyl radical was estimated as ~8.5 eV.  $I$  of 1-methoxycycloheptatrienyl radical was estimated as ~6.2 eV.  $I$  of 1-phenylcycloheptatrienyl radical was assumed to be lower than that of cycloheptatrienyl radical.

in the more polar of the C-R and C-R' bonds. If C-R' is more polar, R' will migrate in preference to R. Accordingly, the quantity  $I_D - A_A$  may constitute an index of the efficiency of photochemical sigmatropic shifts.

**(B) Reactivity Trends of Sigmatropic Shifts.** We now enter the discussion of the experimental evidence pertinent to the above analysis. In the case of thermal nonionic 1,3-sigmatropic shifts, both the retention and inversion pathways involve pericyclic bonding. Accordingly, both stereochemical modes of migration are expected to be stereoselective. However, the inversion pathway involves a lower thermal barrier and, in the absence of steric prohibitions, it may become the preferred path. In short, it is evident that both types of stereochemical results should be expected and, indeed, this has been found to be the case. Thermolysis of compound I has provided an ex-



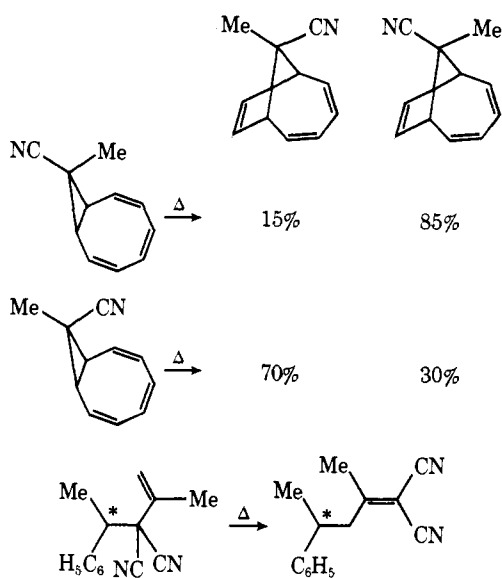
ample of a suprafacial sigmatropic shift proceeding with inversion.<sup>10</sup> On the other hand, reactions occurring by retention of the MG have also been discovered. Typical examples are shown below and more can be found in the literature.<sup>11</sup>

Nonionic photochemical 1,3-sigmatropic shifts are expected to proceed with retention. Cookson<sup>11b</sup> has reported a photochemical polar 1,3-sigmatropic shift which proceeds with retention. Other such photoreactions were found to be non-

Table IV. Toposelectivity of Thermal Sigmatropic Shifts

Compd	Possible products	$I - A$ , eV <sup>e</sup>	Model MG	Model MF	Obsd product
	A	~5.6; ~7.1	MeO $\dot{C}$ H <sub>2</sub>		A <sup>a</sup>
X = OMe, OAc	B	~6.7; >7.1	Me- $\dot{C}$ H <sub>2</sub>		
	A	~5.9; ≥8.7	Me		A <sup>b</sup>
	B	~6.0; ~11	OMe		
	A	~5.6; ~6.05			A <sup>c</sup>
	B	~6.63; ~7.74	Me		
	A	~4.32; ~7.2	Ph- $\dot{C}$ (Me) H		A <sup>d</sup>
	B	~4.9; ~11.6	$\dot{C}$ N		

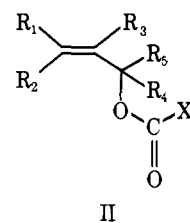
<sup>a</sup>F. Scheidet and W. Kirmse, *J. Chem. Soc., Chem. Commun.*, 716 (1972). <sup>b</sup>H. M. Frey and R. H. Hopkins, *J. Chem. Soc., B*, 1410 (1970). <sup>c</sup>A. Amano and M. Uchiyama, *J. Phys. Chem.*, 69, 1278 (1965). <sup>d</sup>R. C. Cookson and J. E. Kemp, *Chem. Commun.*, 385 (1971). <sup>e</sup>Ionization potential values were taken from D. W. Turner, *Adv. Phys. Org. Chem.*, 4, 30 (1960); electron affinity values were taken from H. O. Pritchard, *Chem. Rev.*, 52, 529 (1952), and from N. S. Husli and J. A. Pople, *Trans. Faraday Soc.*, 51, 600 (1955).  $I$  of 1-methoxyallyl radical was estimated as ~7 eV,  $A$  was assumed to be smaller or equal to that of allyl radical.  $I$  of OMe was assumed to be equal to the oxygen lone pair ionization potential (~13 eV), see: J. H. D. Eland, "Photoelectron Spectroscopy", Butterworths, London, 1974, p 21.  $A$  was approximated as equal to that of OH.  $I$  of Ph-CH(Me) was estimated as ~7.43 eV.  $A$  was approximated as equal to that of Ph-CH<sub>2</sub>.  $I$  of 1,1-dicyanoallyl radical was estimated as 9 eV.  $I$  of CN was taken from: P. J. Wilkinson, *J. Astrophys.*, 138, 778 (1963).  $I$  of 1-cyanoallyl radical was estimated as ~8.6 eV.  $A$  was estimated as 2.6 eV.



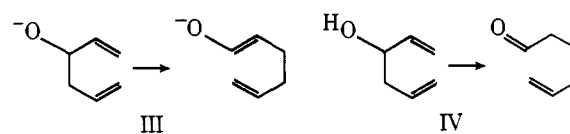
stereoselective and "diradical" mechanisms were proposed.<sup>12</sup> However, nonstereoselectivity may reflect competing pericyclic SR and SI mechanisms. Additional investigations may clarify the situation.

In Table III we list examples of thermal sigmatropic shifts which exhibit lowering of the activation energy as the quantity  $I - A$  decreases. In terms of our theory, only comparisons of systems belonging to the same class are permissible so that interaction matrix elements remain comparable and the polarity rule applicable. Other experimental trends consistent with our predictions are summarized below:

(a) A 1,3 thermal shift of a carboxyl group across an allylic MF becomes faster as R<sub>1</sub>-R<sub>5</sub> become more electron releasing and X more electronegative in II.<sup>13</sup>



(b) The reaction rate of III is 10<sup>10</sup>-10<sup>17</sup> faster than that of IV.<sup>14</sup>



(c) Reactivity patterns in cyclohexadienone chemistry are compatible with the predictions of our theory.<sup>15</sup>

As we have seen before, our theoretical approach lends to the formulation of a simple topochemical rule which can be stated as follows: *a thermal sigmatropic shift will preferentially take place via the path which couples the best donor-acceptor fragments.* In the space below, we provide a simple example of how this rule may be applied.

Consider an intramolecular 1,3-sigmatropic shift occurring in V.



Table V. Toposelectivity of Photochemical Sigmatropic Shifts

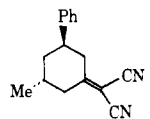
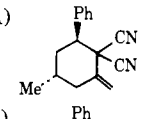
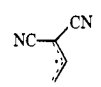
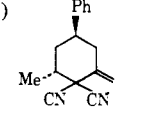
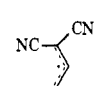
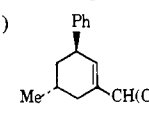
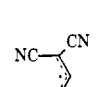
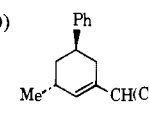
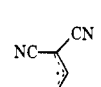
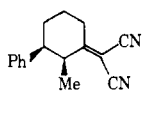
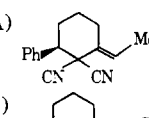
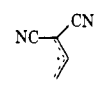
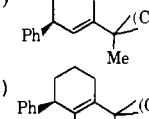
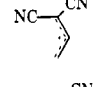
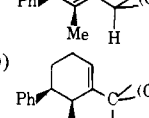
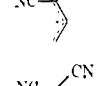
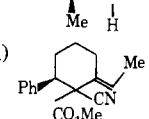
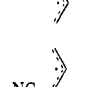
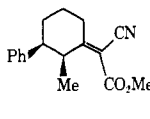
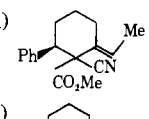
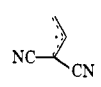
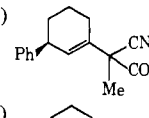
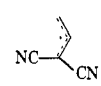
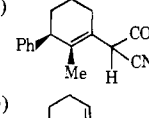
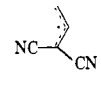
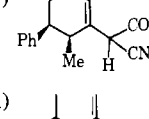
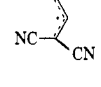
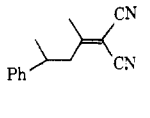
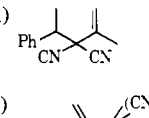
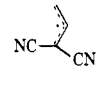
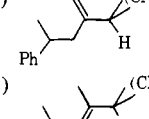
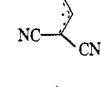
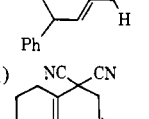
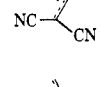
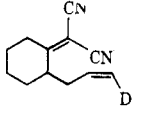
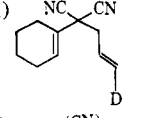

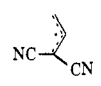
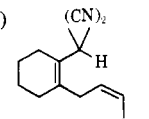
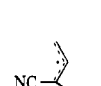
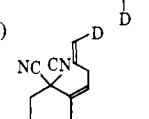
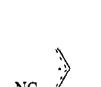
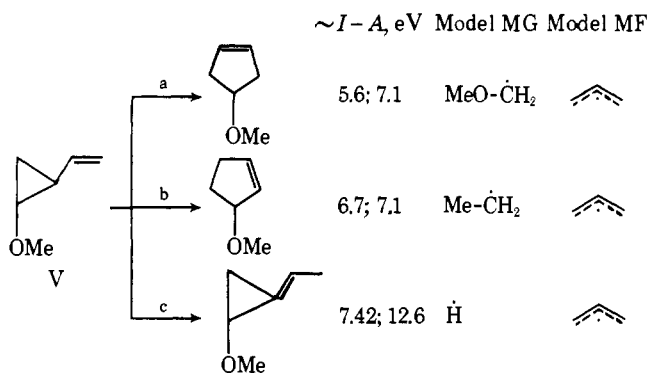
Reactant	Possible products	$I - A, h \text{ eV}$	Model MG	Model MF	Obsd product
	(A) 	~4.6	$\text{Ph}\dot{\text{C}}\text{H}_2$		$A^a$
	(B) 	~5.6	$\text{Me}-\dot{\text{C}}\text{H}_2$		
	(C) 	~10.5	$\dot{\text{H}}$		
	(D) 	~10.5	$\dot{\text{H}}$		
	(A) 	~4.6	$\text{Ph}\dot{\text{C}}\text{H}_2$		$A^b$
	(B) 	~6.7	$\dot{\text{M}}\text{e}$		
	(C) 	~10.5	$\dot{\text{H}}$		
	(D) 	~10.5	$\dot{\text{H}}$		
	(A) 	~4.6	$\text{Ph}\dot{\text{C}}\text{H}_2$		$A^a$
	(B) 	~6.7	$\dot{\text{M}}\text{e}$		
	(C) 	~10.5	$\dot{\text{H}}$		
	(D) 	~10.5	$\dot{\text{H}}$		
	(A) 	~4.3	$\text{Ph}-\dot{\text{C}}\text{H}$ $\quad \quad \quad \text{Me}$		$A^c$
	(B) 	~10.5	$\dot{\text{H}}$		
	(C) 	~10.5	$\dot{\text{H}}$		
	(A) 	~5.0			$A^b$
	(B) 	~10.5	$\dot{\text{H}}$		
	(C) 	~5.6	$\text{Me}-\dot{\text{C}}\text{H}_2$		

Table V (Continued)

Reactant	Possible products	$I - A, {}^h \text{eV}$	Model MG	Model MF	Obsd product
	(D)	~10.5	$\dot{\text{H}}$		
	(A)	~5.2	$\text{Me}_2\dot{\text{C}}$		$A^d$
	(B)	~7.2	$\text{H}_2\dot{\text{C}}^-$		
	(A)	~4.4	$\text{Ph}_2\dot{\text{C}}\text{H}$		$A^e$
	(B)	~5.2	$\text{Ph}_2\dot{\text{C}}\text{H}$		
	(A)	~5.2	$\text{Me}-\dot{\text{C}}\text{O}$		$A^f$
	(B)	~5.9	$\text{Me}-\dot{\text{C}}\text{H}_2$		
	(A)	~6.7	$\text{Me}\dot{\text{C}}\text{O}$		$A^g$
	(B)	~7.3	$\text{Me}$		
	(C)	~7.5	$\dot{\text{H}}$		

<sup>a</sup>R. C. Cookson, J. Hudec, and M. Sharma, *Chem. Commun.*, 107, 108 (1971). <sup>b</sup>R. F. C. Brown, R. C. Cookson, and J. Hudec, *Tetrahedron*, 24, 3955 (1968). <sup>c</sup>R. C. Cookson and J. E. Kemp, *Chem. Commun.*, 385 (1971). <sup>d</sup>J. J. Hurst and G. H. Whitliam, *J. Chem. Soc.*, 2864 (1960). <sup>e</sup>D. W. Boykin, Jr., and R. E. Lutz, *J. Am. Chem. Soc.*, 86, 5046 (1964). <sup>f</sup>R. C. Cookson, A. G. Edwards, J. Hudec, and M. Kingsland, *Chem. Commun.*, 98 (1965). <sup>g</sup>E. Baggiolini, K. Schaffner, and O. Jeger, *Chem. Commun.*, 1103 (1969). <sup>h</sup> $I$  of  $\text{Ph}_2\dot{\text{C}}\text{H}$  and  $A$  of  $\text{Me}\dot{\text{C}}\text{O}$  were taken from: R. R. Zahradnik and P. Carsky, *Prog. Phys. Org. Chem.*, 10, 327 (1973).  $I$  of  $\dot{\text{C}}\text{H}(\text{OMe})_2$  was estimated as ~6.5 eV.

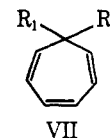
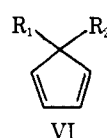


The possible migration pathways are shown along with the quantities  $I - A$ , which constitute measures of the donor-acceptor relationship between MF and MG. For each migration mode, one has to calculate two values of  $I - A$ , one assuming that the MF is the donor and the MG the acceptor and one for the reverse situation. The preferred pathway is (a) because it involves the lowest value of  $I - A$ , i.e., this pathway couples donor and acceptor fragments in the best possible way.

Following similar reasoning, we predict that V will react faster than the unsubstituted derivative which can only undergo a 1,3 shift via a path akin to the inferior path (b). Both these predictions are confirmed by experiment.<sup>16</sup>

In Table IV, we provide examples of the application of the topochemical rule to systems which have been studied experimentally. These data are in agreement with the prediction that a sigmatropic shift will occur via the path which couples the best donor-acceptor combination.

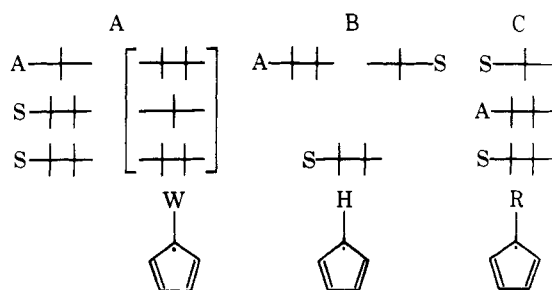
A fascinating example of electronic control of toposselectivity is provided by a comparison of the relative 1,5 migratory aptitudes of  $R_1$  and  $R_2$  placed on cyclic unsaturated rings. A simple prediction can be made by realizing that the MF or VI will act as an *intrinsic* acceptor due to the aromatic nature of  $\text{C}_5\text{H}_5^-$  while the MF of VII will act as an *intrinsic* donor due



to the aromatic nature of  $C_7H_7^+$ . Accordingly, the substituent R to migrate in VI will be the one which has the lowest R-ionization potential. By contrast, the substituent R to remain fixed in VII will be the one which promotes the lowest ( $C_7H_6R$ ) $\cdot$  ionization potential.

The reader should note that the above rules are stated by focusing on ionization potentials rather than electron affinities. This is due to the fact that the former quantities vary more than the latter and, thus, exert primary control on the  $I - A$  index. However, it should be emphasized that the above are rules of thumb. Thus, it is easy to anticipate apparent exceptions when both  $R_1\cdot$  and  $R_2\cdot$  have higher ionization potentials than  $C_5H_5\cdot$  in the case of VI or  $R_1\cdot$  and  $R_2\cdot$  have lower ionization potentials than  $C_7H_7\cdot$  in the case of VII. Accordingly, one should check predictions by explicitly calculating the  $I - A$  indices in each case.

An important point which should be brought to attention concerns the MO degeneracy in cyclic conjugated systems. Thus, as long as the degeneracy of the HO's of the formal cyclic conjugated radicals which constitute the MF is retained or split in a way which allows the singly occupied MO to sustain an electronically favored 1,5-suprafacial shift, the above predictions remain valid. The three possibilities are illustrated by reference to the  $C_5H_4R\cdot$  system.



Only a singly occupied S MO can promote a suprafacial shift. Substituents which promote situation C are effective  $\pi$  donors, while substituents which promote situation A are effective  $\pi$  acceptors. When situations B and C materialize, our previous conclusions are strictly valid. By contrast, in situation A a higher energy configuration (shown in brackets) has to be used for the analysis.

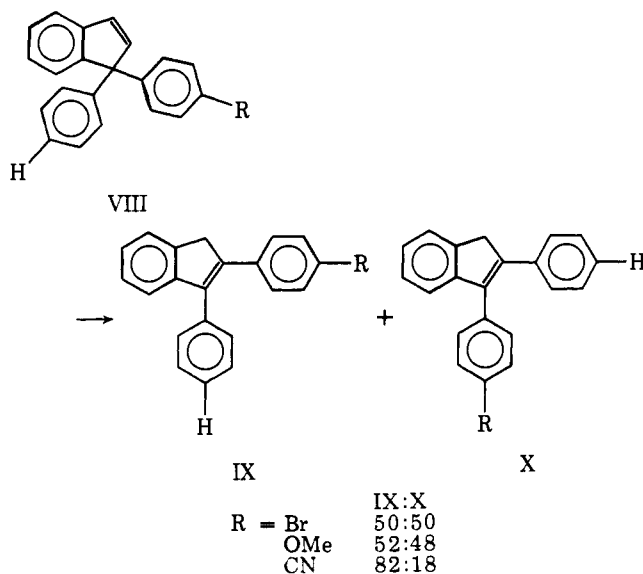
In accordance with expectations based upon the analysis presented above, the following trends have been observed: (a) In  $C_7H_7R$ , where R is a  $\pi$  donor, hydrogen migrates preferentially. As we have seen, the activation energy decreases as  $I - A$  decreases (Table III). (b) In  $C_5H_5R$  ( $R = SiMe_3$ ), the R group migrates preferentially. By contrast, in  $C_7H_7R$  ( $R = SiMe_3$ ), hydrogen migrates preferentially.<sup>17</sup>

An apparent anomaly, the preferred migration of hydrogen in  $C_5H_5CH_3$ , becomes understandable when the  $I - A$  indices are calculated. One anomaly which still persists is the preferred hydrogen migration in  $C_7H_7CN$ .<sup>17</sup>

An interesting example of competition between structurally related groups has been reported. Due to the relatively high ionization potential of the phenyl radical, the 1,5 shifts shown below involve a donor MF and an acceptor MG. Accordingly, it is predicted that IX will become increasingly favored as the electron affinity of the  $RH_4C_5\cdot$  radical increases, i.e., as the

inductive effect of R increases. The experimental results are consistent with this prediction.<sup>17</sup>

The topochemistry of photochemical sigmatropic shifts proceeding in an electronically favored mode can also be predicted by reference to the index  $I_D - A_A$ . In Table V, we pre-



vide examples of photochemical reactions which have been studied experimentally, and which conform to the regiochemical rule. In each case, the preferred mode of migration is the one which couples the MF and MG in the best donor-acceptor combination.

## References and Notes

- (1) See papers 1-4 in this series, N. D. Epiotis and S. Shaik, to be published.
- (2) F. S. Larkin, *Can. J. Chem.*, **46**, 1005 (1968).
- (3) The different terms in eq 1-8 are discussed in ref 1. For additional clarification, see: N. D. Epiotis, *Angew. Chem., Int. Ed. Engl.*, **13**, 751 (1974).
- (4) For a discussion of the static LCGF method, see: N. D. Epiotis, *Angew. Chem., Int. Ed. Engl.*, **13**, 751 (1974).
- (5) The symbol  $N^*$  denotes an intermediate characterized by a wavefunction with a major charge transfer and a minor no-bonding contribution. The subscripts R and P refer to reactant-like and product-like intermediates, respectively.
- (6) The symbol M denotes an intermediate characterized by a wave function with a major charge transfer and a minor local excitation contribution. The subscripts R and P refer to reactant-like and product-like intermediates, respectively.
- (7) In our treatment, the efficiency of radiationless decay processes from an excited to a ground surface is assumed to be a function of the energy gap separating them. However, other factors are involved. For detailed discussions, see: (a) L. Landau, *Phys. Z. Sowjetunion*, **2**, 46 (1932); (b) C. Zener, *Proc. R. Soc. London, Ser. A*, **137**, 696 (1932); (c) G. W. Robinson and R. P. Frosch, *J. Chem. Phys.*, **37**, 1962 (1962); **38**, 1187 (1963); (d) J. Jortner, *Pure Appl. Chem.*, **27**, 389 (1971).
- (8) For similar considerations of solvent effect on the shape of PE surfaces, see: (a) W. G. Dauben, L. Salem, and N. J. Turro, *Acc. Chem. Res.*, **8**, 41 (1975); (b) L. Salem, *Science*, **191**, 822 (1976).
- (9) R. A. Sneath, *Acc. Chem. Res.*, **6**, 46 (1970).
- (10) (a) J. A. Berson and G. L. Nelson, *J. Am. Chem. Soc.*, **89**, 5303 (1967); (b) J. A. Berson, *Acc. Chem. Res.*, **1**, 152 (1968).
- (11) (a) F. G. Klarner, *Tetrahedron Lett.*, 3611 (1971); (b) R. C. Cookson and J. E. Kemp, *Chem. Commun.*, 385 (1971).
- (12) J. Gloor and K. Schaffner, *J. Am. Chem. Soc.*, **97**, 4777 (1975).
- (13) E. S. Lewis, J. T. Hill, and E. R. Newman, *J. Am. Chem. Soc.*, **90**, 662 (1968).
- (14) D. A. Evans and A. M. Golob, *J. Am. Chem. Soc.*, **97**, 4766 (1975).
- (15) B. Miller, *Acc. Chem. Res.*, **8**, 245 (1975).
- (16) J. M. Simpson and H. G. Richey, Jr., *Tetrahedron Lett.*, 2545 (1973).
- (17) C. W. Spangler, *Chem. Rev.*, **76**, 187 (1976).